

Energy Relations of Positron-Electron Pairs Emitted from Surfaces

I. S. Brandt, Z. Wei, and F. O. Schumann*

Max-Planck-Institut für Mikrostrukturphysik, Weinberg 2, D-06120 Halle, Germany

J. Kirschner

Max-Planck Institut für Mikrostrukturphysik, Weinberg 2, 06120 Halle, Germany

and Institut für Physik, Martin-Luther-Universität Halle-Wittenberg, 06099 Halle, Germany

(Received 13 November 2013; revised manuscript received 4 June 2014; published 4 September 2014)

The impact of a primary positron onto a surface may lead to the emission of a correlated positron-electron pair. By means of a lab-based positron beam we studied this pair emission from various surfaces. We analyzed the energy spectra in a symmetric emission geometry. We found that the available energy is shared in an unequal manner among the partners. On average the positron carries a larger fraction of the available energy. The unequal energy sharing is a consequence of positron and electron being distinguishable particles. We provide a model which explains the experimental findings.

DOI: 10.1103/PhysRevLett.113.107601

PACS numbers: 79.60.-i, 71.20.-b

A key aspect of quantum mechanics is the notion of indistinguishable particles. In the case of electrons the total electronic wave function has to be antisymmetric upon exchange (Pauli principle). This does not apply to the case of distinguishable particles, e.g., a positron and an electron which have different charges. Despite the process of annihilation, a sizeable fraction of low primary positrons hitting a surface are elastically backscattered [1–3]. This effect is termed low energy positron diffraction (LEPD) and reveals the surface structure in a similar way to low energy electron diffraction (LEED) [4,5]. The computation of LEED spectra involves exchange effects between the primary electron and the surface electrons [4,5]. This aspect is missing in LEPD, because the positron and electron are distinguishable.

If a primary positron or electron impinges onto a surface, it will interact with the surface electrons leading to an energy loss of the primary particle. The inelastically reemitted primary may be accompanied by the emission of a surface electron. The ejected positron-electron or electron-electron pair can be detected via coincidence techniques. We call this pair emission (p, ep) in the case of positron excitation, while we refer to ($e, 2e$) for primary electron impact. Electron pair emission is, by now, an established technique in atomic, molecular, and solid state physics [6–9]. The possibility to detect the (p, ep) process from surfaces was proven recently [10].

We have demonstrated that a key concept of solid state theory, namely the exchange-correlation hole, is accessible in angular distributions of the ($e, 2e$) intensity [11,12]. A spin-resolved ($e, 2e$) study revealed that it is possible to effectively separate exchange from Coulomb correlation [13,14]. A key ingredient of that work was a ferromagnetic sample. An alternative approach, which does not require ferromagnetic order, is to compare angular (p, ep)

distributions from those of ($e, 2e$) experiments. Because of the lack of exchange in the former, it is possible to disentangle the effect of exchange from the Coulomb correlation. The prospect of this approach was discussed in theoretical (p, ep) studies for surfaces [15,16].

We provide the first evidence that the positron-electron pair production at surfaces leads to features which are a consequence of distinguishable collision partners. This is not a trivial point, because inelastic processes before or after the positron collision may mask the anticipated effect. Our approach is based on general symmetry arguments and their consequence for the energy distributions.

In Fig. 1, we sketch the geometric arrangement of our coincidence experiment. The axis of the primary positron beam, the sample normal, and the lens axes of the “left” and “right” spectrometer form a symmetric arrangement. Let us suppose that an electron pair is emitted in which the electrons possess different kinetic energies E_1 and E_2 , respectively. The likelihood that the electron with energy E_1 is detected by the left spectrometer is identical to being

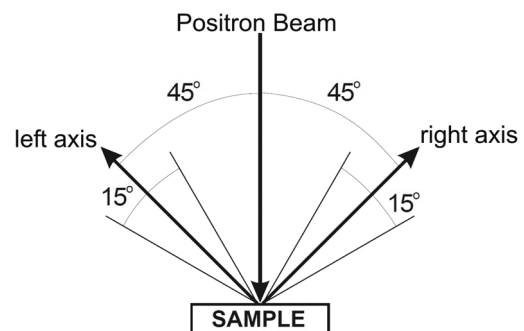


FIG. 1. The two transfer lenses of the spectrometer (with $\pm 15^\circ$ acceptance) are symmetrically aligned with respect to the surface normal. The positron beam is aligned along the surface normal.

registered by the right spectrometer, because electrons can not be distinguished. This symmetry is broken if one of the spectrometers is sensitive to positrons while the other analyzes electrons. Consequently, we have to expect that the energy distributions of positron-electron pairs display a nonsymmetric behavior. A dedicated (p, ep) calculation on a Cu(111) surface using the geometric arrangement presented in Fig. 1 verifies this statement [16]. This argument also holds for a finite angular acceptance which is $\pm 15^\circ$ in our experiment.

With a lab-based positron beam, we studied the positron-pair emission from a Ag(100) surface and a variety of metal and NiO films. The experimental energy distributions clearly show the predicted unequal energy sharing. We discuss our experimental results within a simplified scattering model which qualitatively explains the observed facts.

The details of the coincidence spectrometer can be found elsewhere [10,17,18]. It consists of two hemispherical electron energy analyzers with transfer lenses and angular acceptance $\pm 15^\circ$. Changing the polarity of all electron-optical components allows us to either detect electrons or positrons. We perform (p, ep) experiments with either the left or right spectrometer tuned for positron detection. Recently, we have commissioned a low energy positron source in our laboratory using a Na22 isotope with 50 mCi activity. The emitted positrons have a continuous energy spectrum up to a maximum energy of 545 keV. A positron beam with defined kinetic energy is achieved via the process of moderation [19]. We employ a folded tungsten mesh and the emitted moderated positrons are electrostatically guided into the scattering chamber. The kinetic energy of the positron beam is defined by the potential difference between moderator and sample. A channel plate detector, which can be brought into the measurement position, monitors the primary positron flux. For primary energies in the range of 30–60 eV, we find a flux of 3×10^4 positrons per second. This matches values reported in the literature for electrostatically guided beams.

The spectrometers were set to 300 eV pass energy which results in an energy window of 27 eV covered by each spectrometer in parallel. We use the largest entrance slits and achieve coincidence count rates of a few counts per second. The energy resolution of each spectrometer is 4 eV. The preparation of the Ag(100) surface followed standard procedures of Ar⁺ sputtering and annealing. Metal films were prepared by evaporation at 300 K. NiO films were grown via Ni evaporation in a 10^{-6} mbar O₂ atmosphere. All experiments were performed at room temperature. For sample characterization, equipment for Auger spectroscopy and LEED was available.

We proceed by defining some important parameters. In a (p, ep) process, a primary positron with well-defined primary energy E_p impinges on the surface and a positron-electron pair is emitted. The particles are labeled by a subscript and a superscript which indicates the particle

detected, e.g., if we label the kinetic energies as E_{left}^+ and E_{right}^- , we perform an experiment where the left spectrometer detects positrons while the right spectrometer detects electrons. If we label the polarity of the detected particles with α and β , energy conservation for a (p, ep) experiment reads as

$$E^p + E_{vb} = E_{\text{left}}^\alpha + E_{\text{right}}^\beta + \phi = E_{\text{sum}} + \phi. \quad (1)$$

We remove one electron from the sample, hence, the electron work function ϕ appears. The binding energy E_{vb} is referred to the Fermi level, while the primary energy and the energy of the emitted particles is quoted with respect to the vacuum level of the sample. The positron-electron pair has an energy sum $E_{\text{sum}} = E_{\text{left}}^\alpha + E_{\text{right}}^\beta$, and it has an upper bound given by $E_{\text{sum}}^{\text{max}} = E^p - \phi$. The periodicity of the surface has consequences for the conservation of the in-plane momentum. For normal incidence it simplifies to

$$k_{vb} = k_{\text{left}}^\alpha + k_{\text{right}}^\beta + g. \quad (2)$$

The valence electron momentum is given by k_{vb} while the reciprocal lattice vector is labeled as g . For low energy excitation the reciprocal lattice vector g can be ignored. Usually, the electronic density of states is nonzero over a large part of the surface Brillouin zone. This fact makes it kinematically possible for positron and electron to possess different energies while having emission angles of $\pm 45^\circ$, respectively. This is very different from a binary scattering of positron and electron. Clearly, the existence of the crystal momentum is important for the kinematics.

In Fig. 2, we show two 2D-energy distributions of positron-electron pairs emitted from a Ag(100) surface excited with a 42 eV primary beam. The insets highlight the chosen polarity of the spectrometer. The x axis in both cases is the energy scale mapped by the right spectrometer, while the y axis is the energy of the particles detected with the left spectrometer.

The solid diagonal line in both plots marks the position of the maximum sum energy $E_{\text{sum}}^{\text{max}}$. Essentially no intensity is found above this line. Most of the intensity is found within a triangular shaped region near the lower left hand corner. These events stem from inelastic processes and the energy loss is sufficient to cause the emission of a second electron. Our instrument is not able to record triple coincidences, but we have detected electron pairs due to positron impact. This strongly suggests the existence of triple emission. These are not included in the theoretical description of (p, ep) and have to be excluded in the analysis if we want to invoke the symmetry of the detection geometry. Via appropriate selection of the sum energy, this can be done, and the dashed lines indicate the range considered for the computation of the energy sharing curves, see below.

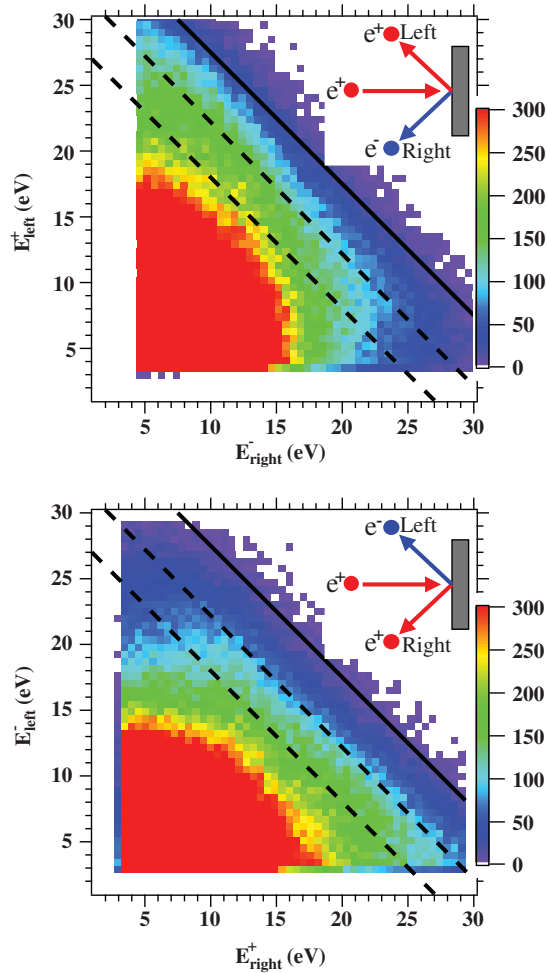


FIG. 2 (color). 2D-energy distribution of positron-electron pairs from Ag(100) surface. The primary energy was 42 eV. The insets indicate which of the particles is detected by the respective spectrometer. The x axis in both plots refers to the energy measured by the “right” spectrometer.

The aforementioned asymmetry in the energy distribution can be seen in Fig. 2(a), if we focus on the region marked by the dashed lines. Within this region the intensity is higher in the upper left-hand region compared to the lower right-hand part. We changed the polarities of the spectrometers and observe, in Fig. 2(b), that the region of higher intensity is now in the lower right-hand corner. This rules out an instrumental asymmetry and proves the existence of a genuine effect.

The dashed lines in Fig. 2 define an energy sum window of $E_{\text{sum}} = 30 \pm 2$ eV. For events in this range, we compute the intensity as a function of the energy difference $E_{\text{left}}^{\alpha} - E_{\text{right}}^{\beta}$. In Fig. 3, we present the result for the (p, ep) experiments together with $(e, 2e)$ data obtained with $E_p = 42$ eV. We clearly observe asymmetric sharing curves for the (p, ep) data, whereas the $(e, 2e)$ spectra are essentially symmetric. This also demonstrates the level of instrumental asymmetry which can be neglected. Changing

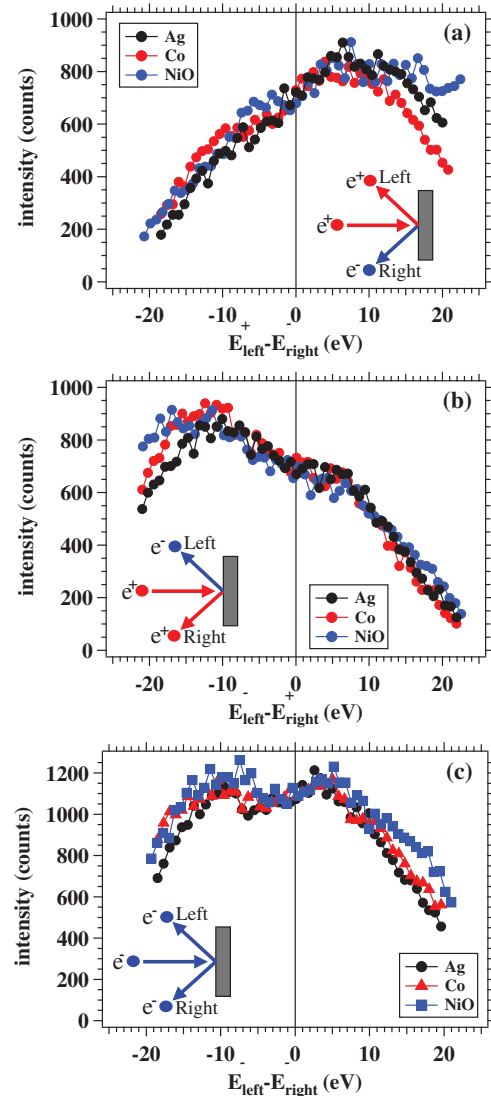


FIG. 3 (color). Energy sharing curves obtained by fixing the sum energy to 30 ± 2 eV. The Ag, Co, and NiO samples were excited by 42 eV positrons. The insets indicate which of the particles is detected by the respective spectrometer. Additionally, we present the curve from the corresponding $(e, 2e)$ experiments.

the polarity of the spectrometers moves the intensity maximum from the right to the left. In Fig. 3(a), most of the intensity is found for positive x values. This means that, on average, the positron has a higher fraction of the available energy. The intensity maxima of the two (p, ep) sharing curves are observed if the positron has 10 eV more energy than the electron. The intensity has the lowest value if the electron has a 20 eV higher energy than the positron. The intensity ratio between these two levels is roughly ≈ 4 . In order to test the generality of these observations, we also investigated single crystalline NiO, Pd, and Fe films. Additionally, we prepared polycrystalline Co, Ni, and Fe films. We have

included the data of Co and NiO in Fig. 3. For the purpose of comparison, we scaled the intensity of the Co and NiO data such that they line up for equal energy sharing with the Ag data.

An effective single particle picture works well to describe the material properties of Ag. Co and NiO both display long range order, this is a manifestation of electron correlation via the exchange interaction. NiO is an insulator, a property decisively determined by the electron correlation. Despite these differences, the amount of the asymmetry in the sharing curves varies slightly between the materials. Common to these samples is that, on average, the positron carries more energy than the electron. Although the sharing curves closely resemble each other, the actual coincidence count rates differ strongly between these materials as seen in (e , $2e$) experiments [20].

Our observations were not *a priori* expected, because the theoretical (p , ep) studies predict that either the electron or the positron is the more energetic particle [15,16]. Details of the valence band structure determine the outcome, but no simple argument can be put forward.

Our results can be qualitatively explained by a simplified scattering model. If we ignore the solid state environment for the moment, it reduces to a two-body problem. In the laboratory frame, the electron is initially at rest, while the primary positron approaches it with primary energy E_p . Afterwards, the positron has lost part of its energy to the electron and is deflected by an angle ϑ from its original trajectory, see Fig. 4. The electron has a momentum direction characterized by an angle φ with respect to the momentum of the primary positron. Energy and momentum conservation uniquely define the energies of the two particles and the propagation direction of the electron for a given value of ϑ . Straightforward evaluation of the energy and momentum conservation leads to terms of the kinetic

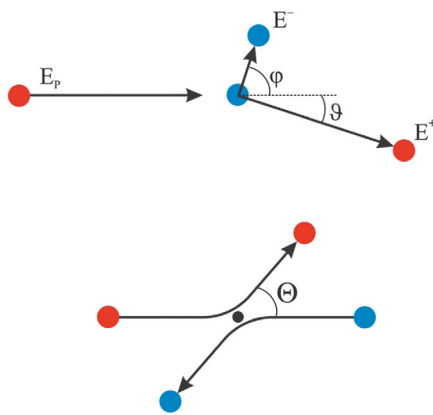


FIG. 4 (color). The collision between positron (red) and electron (blue) in the laboratory and center-of mass frame. In the laboratory frame, the electron is initially at rest. The angles ϑ and φ characterize the propagation direction after the scattering. For equal mass particles, it is known that $\vartheta + \varphi = 90^\circ$ and $\Theta = 2\vartheta$.

energy of positron $E^+(\vartheta)$ and electron $E^-(\vartheta)$ after the collision. This, finally, leads for the energy difference or energy sharing ΔE

$$\Delta E = E^+(\vartheta) - E^-(\vartheta) = E_p \cos(2\vartheta). \quad (3)$$

The actual scattering problem is usually calculated after transformation into the center-of-mass frame, see Fig. 4. For equal mass particles, the relation between the scattering angles in the two reference frames is given by $\Theta = 2\vartheta$. This angle occurs already in the expression for ΔE , see Eq. (3). The theoretical description of the (p , ep) and (e , $2e$) process at solid surfaces assumes a screened Coulomb interaction between the collision partners [16,21,22]. For a numerical example, we set the kinetic energy of the primary positron to 30 eV, while the screening length is 2 Å. This reflects values used in a (p , ep) calculation for a Cu(111) surface [16]. For further analysis we use the 1st Born approximation to determine the scattering amplitude $f(\Theta)$. With this, we know the probability for a particular energy sharing to occur. This probability of the sharing we use for the surface scattering without relating the angles ϑ and φ to the emission angles covered by our spectrometers. This step takes into account the less stringent kinematics in the surface scattering as discussed before. In Fig. 5, we compare the model sharing curve with the experimental result plotted in Fig. 3. The model calculation predicts a monotonic increase of the intensity as a function of $E^+ - E^-$. For energy sharings $|E^+ - E^-| \leq 10$, a rather good agreement to the experiment is given. For larger absolute energy sharing, the experimental intensity is below the model calculation. Clearly, our model can not replace a dedicated (p , ep) calculation. Nevertheless, the actual positron-electron collision will lead to the preference for the positron to have more energy than the electron.

A consequence of the binary scattering geometry of Fig. 4 is that, in the laboratory frame, both particles must have momentum components along the forward direction.

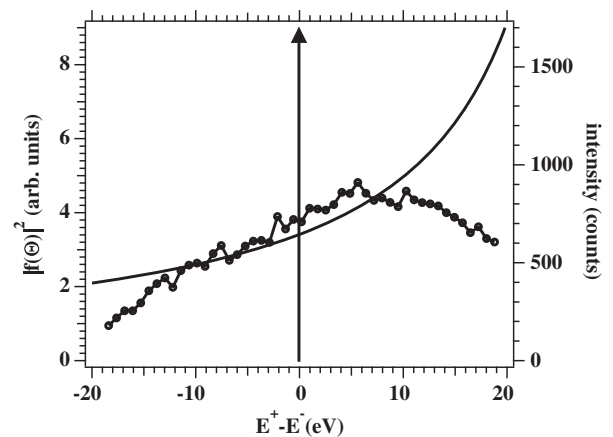


FIG. 5. We present the sharing distribution $E^+ - E^-$ using Eq. (3) together with the data of Ag shown in Fig. 3(a).

This is clearly different from our experimental geometry where the particles have momentum components along the backward direction. These two scenarios can be reconciled if we recall the existence of LEPD [1–3]. It is the reflected beam which acts as the primary beam for the positron-electron scattering.

The presented sharing curves focussed on an energy window bounded by the dashed diagonal lines in Fig. 2. However, the sharing curves for other values of the sum energy also display an asymmetric shape.

In summary we performed positron-electron pair emission experiments from surfaces. For a symmetric emission geometry, we observed that the available energy is shared unequally among the partners. This is a consequence of the fact that positron and electron are distinguishable. The asymmetric sharing is rather strong and is independent of the material studied. We find that, on average, the positron carries more energy than the electron for the materials studied. We provided a simple model of the positron-electron scattering which corroborates the findings qualitatively.

The development of the positron beam benefited from the suggestions of R. Krause-Rehberg and P. Coleman. We took advantage of stimulating discussions with H. Gollisch, F. Giebels, and R. Feder. We thank the iThemba team for support and hospitality during the positron source characterization. Funding from the DFG through SFB 762 is gratefully acknowledged.

*schumann@mpi-halle.de

- [1] I. J. Rosenberg, A. H. Weiss, and K. F. Canter, *Phys. Rev. Lett.* **44**, 1139 (1980).
- [2] A. H. Weiss, I. J. Rosenberg, K. F. Canter, C. B. Duke, and A. Paton, *Phys. Rev. B* **27**, 867 (1983).
- [3] X. M. Chen, K. F. Canter, C. B. Duke, A. Paton, D. L. Lessor, and W. K. Ford, *Phys. Rev. B* **48**, 2400 (1993).
- [4] R. Feder, *Solid State Commun.* **34**, 541 (1980).
- [5] C. B. Duke, A. Paton, A. Lazarides, D. Vasumathi, and K. F. Canter, *Phys. Rev. B* **55**, 7181 (1997).
- [6] H. Ehrhardt, M. Schulz, T. Tekaats, and K. Willmann, *Phys. Rev. Lett.* **22**, 89 (1969).
- [7] R. Camilloni, A. G. Guidoni, R. Tiribelli, and G. Stefani, *Phys. Rev. Lett.* **29**, 618 (1972).
- [8] I. E. McCarthy and E. Weigold, *Phys. Rep.* **27**, 275 (1976).
- [9] J. Ullrich, R. Moshhammer, A. Dorn, R. Dörner, L. P. H. Schmidt, and H. Schmidt-Böcking, *Rep. Prog. Phys.* **66**, 1463 (2003).
- [10] G. A. van Riessen, F. O. Schumann, M. Birke, C. Winkler, and J. Kirschner, *J. Phys. Condens. Matter* **20**, 442001 (2008).
- [11] F. O. Schumann, J. Kirschner, and J. Berakdar, *Phys. Rev. Lett.* **95**, 117601 (2005).
- [12] F. O. Schumann, C. Winkler, and J. Kirschner, *Phys. Rev. Lett.* **98**, 257604 (2007).
- [13] F. O. Schumann, C. Winkler, J. Kirschner, F. Giebels, H. Gollisch, and R. Feder, *Phys. Rev. Lett.* **104**, 087602 (2010).
- [14] F. Giebels, H. Gollisch, R. Feder, F. O. Schumann, C. Winkler, and J. Kirschner, *Phys. Rev. B* **84**, 165421 (2011).
- [15] J. Berakdar, *Nucl. Instrum. Methods Phys. Res., Sect. B* **171**, 204 (2000).
- [16] F. Giebels, H. Gollisch, and R. Feder, *J. Phys. Condens. Matter* **21**, 355002 (2009).
- [17] G. A. van Riessen, Z. Wei, R. S. Dhaka, C. Winkler, F. O. Schumann, and J. Kirschner, *J. Phys. Condens. Matter* **22**, 092201 (2010).
- [18] F. O. Schumann, R. S. Dhaka, G. A. van Riessen, Z. Wei, and J. Kirschner, *Phys. Rev. B* **84**, 125106 (2011).
- [19] P. J. Schultz and K. G. Lynn, *Rev. Mod. Phys.* **60**, 701 (1988).
- [20] F. O. Schumann, L. Behnke, C. H. Li, J. Kirschner, Y. Pavlyukh, and J. Berakdar, *Phys. Rev. B* **86**, 035131 (2012).
- [21] U. Rucker, H. Gollisch, and R. Feder, *Phys. Rev. B* **72**, 214424 (2005).
- [22] H. Gollisch, N. v. Schwartzberg, and R. Feder, *Phys. Rev. B* **74**, 075407 (2006).